AIAA JOURNAL
Vol. 35, No. 7, July 1997

Unsteady Transonic Flow: Flow About a Suddenly Deflected Wedge

Julian D. Cole*
Rensselaer Polytechnic Institute, Troy, New York 12180
and
L. Pamela Cook† and Gilberto Schleiniger‡
University of Delaware, Newark, Delaware 19716

Analysis of unsteady transonic flows is important in the understanding of maneuvering and accelerating flight near the speed of sound. The flow about a suddenly deflected two-dimensional wedge is investigated. Asymptotic methods are used to develop the appropriate unsteady transonic small-disturbance formulation. Numerical calculations are presented and discussed that show the development of shock patterns and the approach to steady state for flows with Mach numbers in the neighborhood of 1.

Introduction

IN this paper, the flow about a suddenly deflected wedge in a uniform stream with upstream Mach number M_∞ near 1 is studied. Asymptotic methods are used to develop the appropriate unsteady transonic small disturbance formulation of the problem on which numerical computation is then carried out. The development of the shock patterns and the approach to steady state is shown in cases where $M_\infty < 1$ (subsonic), $M_\infty = 1$ (sonic), and $M_\infty > 1$ (supersonic), where $M_\infty = U/a_\infty$ is the upstream Mach number for the flow and a_∞ is the speed of sound in the undisturbed gas.

Consider a uniform steady flow in the $x*$ direction for $t* < 0$ (and for $t* > 0$ at upstream infinity) with speed $U \approx a_\infty$. At $t* = 0$, a wedge, originally the line $x* > 0$, $y* = 0$, opens to an angle $\delta \ll 1$ so that for $t* > 0$ the wedge is located at $y* = \pm\delta x*$, $x* > 0$. Because the problem is symmetric about $y* = 0$, we consider only $y* \geq 0$ henceforth, and the vertical velocity at $y* = 0$ is zero for $x* < 0$.

To study this problem, we note that, because the shocks are weak, the flow is isentropic with small corrections so that a potential, $\Phi(x*, y*, t*)$, describes the primary flow. The full two-dimensional potential formulation is[1]

$$(a^2 - \Phi_{x*}^2)\Phi_{x*x*} - 2\Phi_{x*}\Phi_{y*}\Phi_{x*y*} + (a^2 - \Phi_{y*}^2)\Phi_{y*y*}$$
$$- 2\Phi_{x*}\Phi_{x*t*} - 2\Phi_{y*}\Phi_{y*t*} - \Phi_{t*t*} = 0 \tag{1}$$

where a, the local speed of sound, is given by

$$\Phi_{t*} + \frac{a^2}{\gamma - 1} + \frac{\Phi_{x*}^2 + \Phi_{y*}^2}{2} = \frac{a_\infty^2}{\gamma - 1} + \frac{U^2}{2} \tag{2}$$

The boundary conditions are

$$H(\zeta) = \begin{cases} 1 & \text{if} \quad \zeta \geq 0 \\ 0 & \text{if} \quad \zeta < 0 \end{cases}$$

$$\Phi \to Ux* \quad \text{as} \quad x* \to -\infty \tag{3}$$

$$\Phi_{y*}(x*, 0) = 0 \quad \text{if} \quad x* < 0 \tag{4}$$

$$\Phi_{y*}(x*, \delta x*) = \delta\Phi_{x*}(x*, \delta x*)H(t*) \quad \text{if} \quad x* > 0 \tag{5}$$

where H is the Heaviside function. We first study the predictions of linear theory to find where and how it breaks down. That information then guides the development and description of the nonlinear theory.

Received Sept. 20, 1996; revision received March 6, 1997; accepted for publication March 6, 1997.

*Professor, Department of Mathematical Sciences. Fellow AIAA.
†Professor, Department of Mathematical Sciences. Member AIAA.
‡Associate Professor, Department of Mathematical Sciences.

Linear Theory

Linear theory results after nondimensional scaling $t* = (\ell/U)t$, $x* = \ell x$, $y* = \ell y$ (where ℓ is a length scale), from an asymptotic expansion in terms of $\delta \ll 1$:

$$\Phi(x*, y*, t*) = U\ell\{x + \delta\phi(x, y, t) + \cdots\}$$

Substitution into Eqs. (1–5), and collection of terms of corresponding orders, gives to order δ,

$$(M_\infty^2 - 1)\phi_{xx} - \phi_{yy} + 2M_\infty^2\phi_{xt} + M_\infty^2\phi_{tt} = 0$$
$$\phi_y\big|_{y=0} = H(x)H(t)$$
$$\phi_x \sim 0 \quad \text{as} \quad x \to -\infty$$

A change of coordinates to

$$x' = x - t \quad \text{and} \quad \bar{t} = t/M_\infty$$

gives the following problem for the wave equation:

$$\phi_{x'x'} + \phi_{yy} - \phi_{\bar{t}\bar{t}} = 0$$

with

$$\phi_y\big|_{y=0} = H(x' + M_\infty\bar{t})H(\bar{t})$$

and

$$\phi_{x'} \sim 0 \quad \text{as} \quad x' \to -\infty$$

This wave equation corresponds to the propagation of acoustic waves with speed one in a coordinate system moving with the freestream flow (see Fig. 1 for the case $M_\infty < 1$).

The solution to this problem is

$$\phi = \frac{-1}{\pi}\iint_{\mathcal{D}} \frac{H(\xi + M_\infty\tau)}{\sqrt{(\bar{t} - \tau)^2 - (x' - \xi)^2 - y^2}}\, d\xi\, d\tau \quad \text{for} \quad x'^2 + y^2 < \bar{t}^2$$

$$\phi = (y - \bar{t})H(x')H(\bar{t} - y) \quad \text{for} \quad x'^2 + y^2 \geq \bar{t}^2$$

except when $M_\infty > 1$, in which case also

$$\phi = y - \frac{x' + M_\infty\bar{t}}{\sqrt{M_\infty^2 - 1}} \quad \text{for} \quad 0 < y < \frac{\bar{t}}{M_\infty}\sqrt{M_\infty^2 - 1}$$
$$\sqrt{M_\infty^2 - 1}\,y - M_\infty\bar{t} < x' < -\sqrt{\bar{t}^2 - y^2}$$

Note that the domain of integration $\mathcal{D}$ is the region bounded by the wedge, the $y = 0$ axis, and the retrograde Mach cone. This

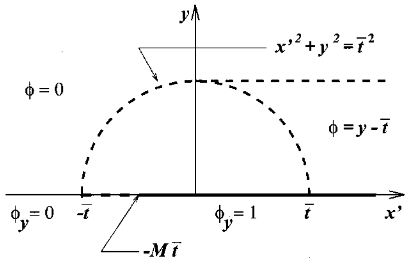

Fig. 1 Acoustic waves: $M_\infty < 1$.

can be integrated out directly to give, for $x'^2 + y^2 < \bar{t}^2$ (in x, t, $\bar{t}$ variables),

$$
\begin{aligned}
-\pi\phi = {} & \bar{t}\left[\sin^{-1}\left(\frac{x-t}{\sqrt{\bar{t}^2-y^2}}\right)+\frac{\pi}{2}\right] \\
& - y\left[\sin^{-1}\left(\frac{\bar{t}(x+\bar{t}-t)-y^2}{(x-t+\bar{t})\sqrt{\bar{t}^2-y^2}}\right)+\frac{\pi}{2}\right] \\
& - y\left[\sin^{-1}\left(\frac{(1-M_\infty)y^2+x(x+\bar{t}-t)}{(x+\bar{t}-t)\sqrt{x^2+(1-M_\infty^2)y^2}}\right)-\frac{\pi}{2}\right] \\
& + \frac{x}{\sqrt{1-M_\infty^2}}\left\{\ln\left|\sqrt{(M_\infty^2-1)[(x-t)^2+y^2-\bar{t}^2]}\right.\right. \\
& \left.\left. + M_\infty(x-t)+\bar{t}\right| - \ln\sqrt{x^2+(1-M_\infty^2)y^2}\right\}
\end{aligned}
\tag{6}
$$

if $M_\infty < 1$;

$$
\begin{aligned}
-\pi\phi = {} & \bar{t}\left[\sin^{-1}\left(\frac{x-t}{\sqrt{\bar{t}^2-y^2}}\right)+\frac{\pi}{2}\right] \\
& - y\left[\sin^{-1}\left(\frac{\bar{t}(x+\bar{t}-t)-y^2}{(x+\bar{t}-t)\sqrt{\bar{t}^2-y^2}}\right)+\frac{\pi}{2}\right] \\
& + y\left[\sin^{-1}\left(\frac{x(x-t+\bar{t})-(M_\infty-1)y^2}{(x-t+\bar{t})\sqrt{x^2-(M_\infty^2-1)y^2}}\right)-\frac{\pi}{2}\right] \\
& - \frac{x}{\sqrt{M_\infty^2-1}}\left[\sin^{-1}\left(\frac{M_\infty x+\bar{t}-M_\infty t}{\sqrt{x^2-(M_\infty^2-1)y^2}}\right)-\frac{\pi}{2}\right]
\end{aligned}
\tag{7}
$$

if $M_\infty > 1$; and

$$
\begin{aligned}
-\pi\phi = {} & \sqrt{x(2t-x)-y^2} + t\left[\frac{\pi}{2}+\sin^{-1}\left(\frac{x-t}{\sqrt{t^2-y^2}}\right)\right] \\
& - y\left[\frac{\pi}{2}+\sin^{-1}\left(\frac{tx-y^2}{x\sqrt{t^2-y^2}}\right)\right]
\end{aligned}
\tag{8}
$$

if $M_\infty = 1$. Note that because

$$\arcsin x = -i\,\mathcal{L}n[\sqrt{1-x^2}+ix] \qquad \text{if} \qquad x^2 \leq 1$$

Equations (6) and (7) agree and, furthermore, as $M_\infty \to 1$, for x, y fixed, $x \neq 0$, Eqs. (6) and (7) become Eq. (8).

Note that linearized theory breaks down for $M_\infty \approx 1$ because, in x', $\bar{t}$ coordinates, the wedge is flying at Mach 1 so that disturbances pile up at the nose, eventually forming a shock. Nonlinear theory must be used to correctly represent the interactions at this point in recognition of the fact that disturbances in the flow direction are of much larger order than those occurring transversely.

Nonlinear Theory

In the nonlinear theory, we look for $\mu(\delta)$, $\nu(\delta)$, $\epsilon(\delta)$, $\sigma(\delta)$, so that

$$\Phi(x*, y*, t*) = U\ell\{x + \epsilon(\delta)\varphi(\tilde{x}, \tilde{y}, t; K) + \dots\}$$

where $\tilde{x}$, $\tilde{y}$ are stretched coordinates

$$\tilde{x} = x/\mu(\delta), \qquad \tilde{y} = y/\nu(\delta) \qquad \text{and} \qquad K = (1-M_\infty^2)/\sigma(\delta)$$

Note that K will be $>$, $=$, or $<$ 0 in what follows as M_∞ is $<$, $=$, or >1. Determination of ϵ, μ, ν, and σ is made by insisting that the boundary condition be retained $[\Phi_{y*}|_{y*=0} = U(\epsilon/\nu)\phi_{\tilde{y}}|_{\tilde{y}=0} = O(\delta)]$, that the nonlinear term in the flow direction be preserved as well as the transonic nature of the equation, and that the unsteady nature of the problem be maintained. Hence, $\nu = \delta^{1/3}$, $\mu = \delta^{2/3}$, $\epsilon = \delta^{4/3}$, and $\sigma = \delta^{2/3}$, so that

$$\Phi = U\ell\{x + \delta^{\frac{4}{3}}\varphi(\tilde{x}, \tilde{y}, t; K) + \dots\}$$

where

$$K = \frac{1-M_\infty^2}{\delta^{\frac{2}{3}}}, \qquad \tilde{x} = \frac{x}{\delta^{\frac{2}{3}}}, \qquad \tilde{y} = \frac{y}{\delta^{\frac{1}{3}}}$$

and φ is governed by the unsteady transonic small disturbance equation

$$(K - (\gamma+1)\varphi_{\tilde{x}})\varphi_{\tilde{x}\tilde{x}} + \varphi_{\tilde{y}\tilde{y}} - 2\varphi_{\tilde{x}t} = 0 \tag{9}$$

with

$$\varphi_{\tilde{y}}|_{\tilde{y}=0} = H(\tilde{x})H(t) \tag{10}$$

In addition, for $M_\infty < 1$

$$
\begin{aligned}
-\pi\varphi \sim {} & \sqrt{2t\tilde{x}+Kt^2-\tilde{y}^2} \\
& - \tilde{y}\left[\sin^{-1}\left(\frac{\tilde{x}(2\tilde{x}+Kt)+K\tilde{y}^2}{(2\tilde{x}+Kt)\sqrt{\tilde{x}^2+K\tilde{y}^2}}\right)\right. \\
& \left. + \sin^{-1}\left(1-\frac{2\tilde{y}^2}{t(2\tilde{x}+Kt)}\right)\right] \\
& + \frac{\tilde{x}}{\sqrt{K}}\left[\ln\left|\sqrt{K(2\tilde{x}t+Kt^2-\tilde{y}^2)}+\tilde{x}+Kt\right|\right. \\
& \left. - \ln\sqrt{\tilde{x}^2+K\tilde{y}^2}\right] \qquad \text{for} \qquad \tilde{y}^2 < 2\tilde{x}t+Kt^2 \\
\sim {} & 0 \qquad \text{for} \qquad \tilde{y}^2 > 2\tilde{x}t+Kt^2
\end{aligned}
\tag{11}
$$

or, for $M_\infty > 1$,

$$
\begin{aligned}
-\pi\varphi \sim {} & \sqrt{2\tilde{x}t+Kt^2-\tilde{y}^2} \\
& - \tilde{y}\left[-\sin^{-1}\left(\frac{\tilde{x}(2\tilde{x}+Kt)+K\tilde{y}^2}{(2\tilde{x}+Kt)\sqrt{\tilde{x}^2+K\tilde{y}^2}}\right)\right. \\
& \left. + \sin^{-1}\left(1-\frac{2\tilde{y}^2}{t(2\tilde{x}+Kt)}\right)+\pi\right] \\
& - \frac{\tilde{x}}{\sqrt{|K|}}\left[\sin^{-1}\left(\frac{\tilde{x}+Kt}{\sqrt{\tilde{x}^2+K\tilde{y}^2}}\right)-\frac{\pi}{2}\right] \\
& \text{for} \qquad \tilde{y}^2 < 2\tilde{x}t+Kt^2 \\
\sim {} & 0 \qquad \text{for} \qquad \tilde{y}^2 > 2\tilde{x}+Kt^2
\end{aligned}
\tag{12}
$$

or, for $M_\infty = 1$,

$$
\begin{aligned}
-\pi\varphi \sim {} & 2\sqrt{2\tilde{x}t-\tilde{y}^2} - \tilde{y}\{(\pi/2)+\sin^{-1}[1-(\tilde{y}^2/t\tilde{x})]\} \\
& \text{for} \qquad t > 0, \qquad (\tilde{y}^2/\tilde{x}t) < 2 \text{ fixed} \\
\sim {} & 0 \qquad \text{otherwise}
\end{aligned}
\tag{13}
$$

as $\tilde{x}, \tilde{y} \to \infty$.

The far-field condition was obtained by matching with the near-field linear solutions obtained from Eqs. (6–8).

Note that $\delta\phi(x, y, t) \sim \delta^{4/3}\varphi(\tilde{x}, \tilde{y}, t)$. Note also that this matching does in fact determine the scale of the nonlinear stretching. Instead of the conditions we used to determine ϵ, μ, ν, and σ, we could have used the necessity for matching. Thus from Eq. (8), we would have required $\delta\sqrt{[\mu(\delta)]} = \delta\nu(\delta) = \epsilon(\delta)$, giving $\mu = \nu^2$. Because $\epsilon = \nu\delta$ (from the boundary condition on the wedge), ϵ, μ, ν, and σ are determined with only one other condition, namely that Eq. (9) be a distinguished limit of Eq. (1). Note also that, although the transonic correction to the uniform flow is $O(\delta^{4/3})$, the transonic correction to the pressure is in fact $O(\delta^{2/3})$.

Conical Coordinates

The nonlinear problem (9–13), to be solved numerically to determine the nonlinear effects, involves three independent variables. This boundary value problem has conical symmetry. We could thus use the conical coordinates

$$X = \tilde{x}/t, \qquad Y = \tilde{y}/t, \qquad \varphi(\tilde{x}, \tilde{y}, t) = t\psi(X, Y)$$

to study the problem. But, in fact, it is useful to make yet one more change of variables,[2–4] namely to let $R = X - Y^2/2 + K/2$ and $\vartheta = Y$. In these coordinates, the mixed derivative term disappears from the equation. Thus, we get the mixed type equation

$$[(\gamma+1)\psi_R - 2R]\psi_{RR} - \psi_{\vartheta\vartheta} + \psi_R = 0 \tag{14}$$

with

$$\psi_\vartheta|_{\vartheta=0} = H(R - K/2) \tag{15}$$

and

$$\begin{aligned}\psi \sim \frac{-1}{\pi} H(R)\Bigg\{ & \sqrt{2R} + \frac{2R + \vartheta^2 - K}{2\sqrt{K}} \\ & \times \Big[\ell n\left|2\sqrt{2KR} + 2R + \vartheta^2 + K\right| \\ & - \ell n\sqrt{(2R + \vartheta^2 - K)^2 + 4K\vartheta^2}\Big] \\ & - \vartheta\Bigg[\sin^{-1}\left(\frac{2R - \vartheta^2}{2R + \vartheta^2}\right) \\ & + \sin^{-1}\left(\frac{(2R + \vartheta^2)^2 - K(2R - \vartheta^2)}{(2R + \vartheta^2)\sqrt{(2R + \vartheta^2 - K)^2 + 4K\vartheta^2}}\right)\Bigg]\Bigg\}\end{aligned} \tag{16}$$

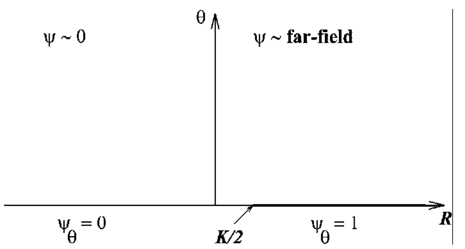

Fig. 2 Boundary and far-field conditions: $M_\infty < 1$.

if $M_\infty < 1$ (see Fig. 2),

$$\begin{aligned}\psi \sim -\frac{1}{\pi} H(R)\Bigg\{ & \sqrt{2R} - \frac{2R + \vartheta^2 - K}{2\sqrt{|K|}} \\ & \times \left[\sin^{-1}\left(\frac{2R + \vartheta^2 + K}{\sqrt{(2R + \vartheta^2 - K)^2 + 4K\vartheta^2}}\right) - \frac{\pi}{2}\right] \\ & - \vartheta\Bigg[\sin^{-1}\left(\frac{2R - \vartheta^2}{2R + \vartheta^2}\right) \\ & - \sin^{-1}\left(\frac{(2R + \vartheta^2)^2 - K(2R - \vartheta^2)}{(2R + \vartheta^2)\sqrt{(2R + \vartheta^2 - K)^2 + 4K\vartheta^2}}\right) + \pi\Bigg]\Bigg\}\end{aligned} \tag{17}$$

if $M_\infty > 1$, and

$$\psi \sim -\frac{1}{\pi} H(R)\left\{2\sqrt{2R} - \vartheta\left[\sin^{-1}\left(\frac{2R - \vartheta^2}{2R + \vartheta^2}\right) + \frac{\pi}{2}\right]\right\} \tag{18}$$

if $M_\infty = 1$ [which is in fact just the limit of Eq. (16) or (17) as $K \to 0$] as R, $\vartheta \to \infty$.

In these coordinates, one finds the slopes of the characteristics and shocks as

$$\left(\frac{\mathrm{d}R}{\mathrm{d}\vartheta}\right)_{\text{characteristic}} = \pm\sqrt{(\gamma+1)\psi_R - 2R}$$

$$\left(\frac{\mathrm{d}R}{\mathrm{d}\vartheta}\right)_{\text{shock}} = \pm\sqrt{(\gamma+1)\langle\psi_R\rangle - 2R}$$

where $\langle\,\rangle$ denotes the average across the shock. The latter came from the shock jump conditions, which are

$$[\![\psi]\!] = 0$$

and

$$[\![(\gamma+1)\psi_R^2/2 - 2R\psi_R]\!]\,\mathrm{d}\vartheta + [\![\psi_\vartheta]\!]\,\mathrm{d}R = 0$$

Here $[\![\;]\!]$ denotes the jump across the shock. Thus, the shock polar is

$$\{(\gamma+1)\langle\psi_R\rangle - 2R\}[\![\psi_R]\!] = [\![\psi_\vartheta]\!]^2$$

Conclusions

The numerical solution of Eqs. (14–18), coupled with the shock jump conditions, was found by using a type-sensitive, conservative finite-difference scheme. The pressure coefficient plots, Figs. 3–18, show the shock development. These plots also show the stagnation point singularity at the nose of the wedge and how the shock forms.

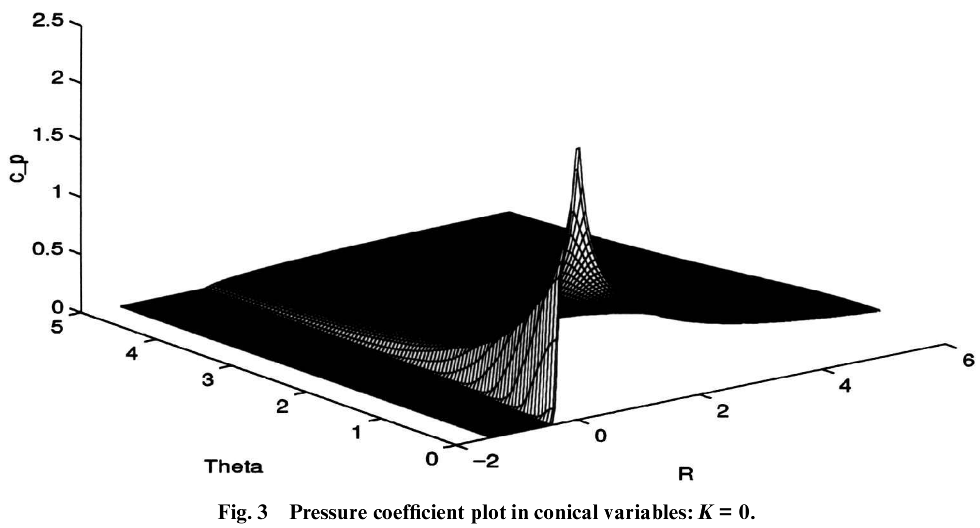

Fig. 3 Pressure coefficient plot in conical variables: $K = 0$.

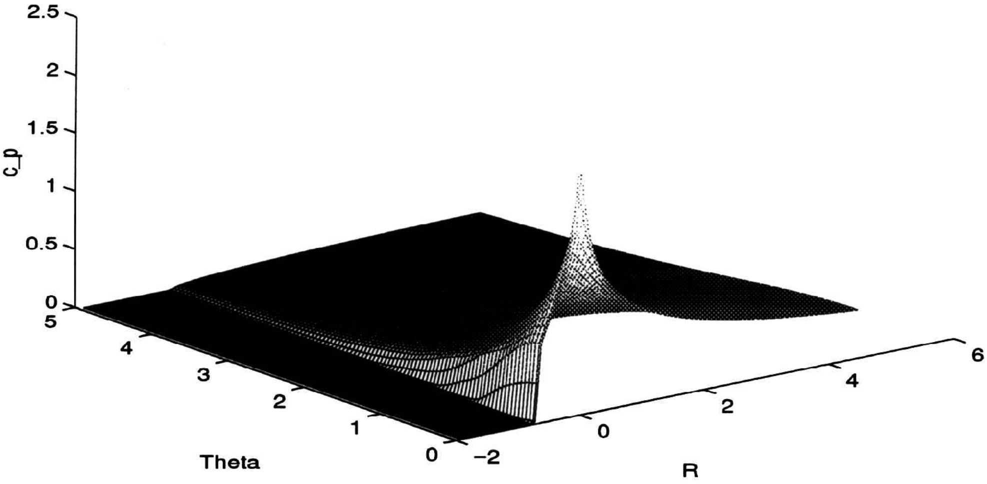

Fig. 4 Pressure coefficient plot in conical variables: *K* = 1.

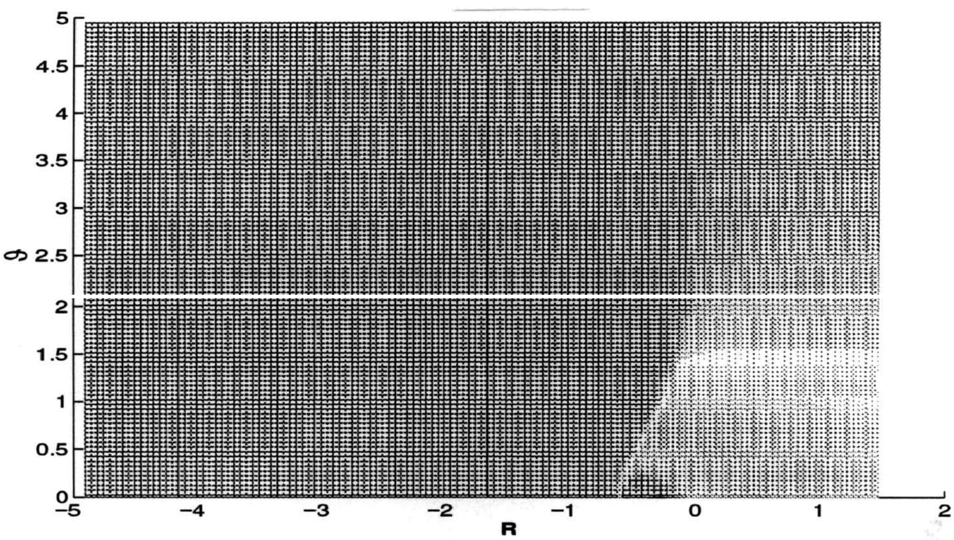

Fig. 5 Pressure coefficient contours in conical variables: *K* = _1.

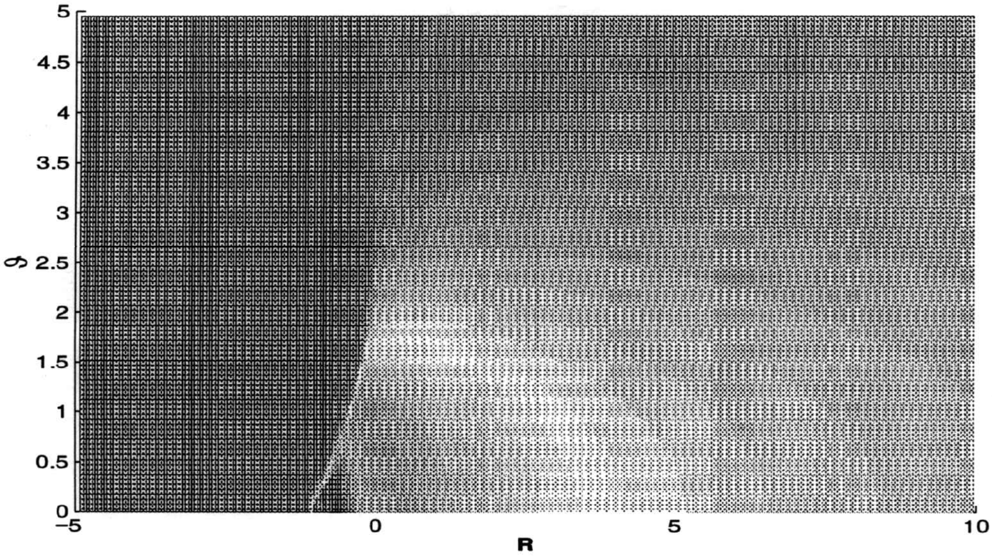

Fig. 6 Pressure coefficient contours in conical variables: *K* = _2.134.

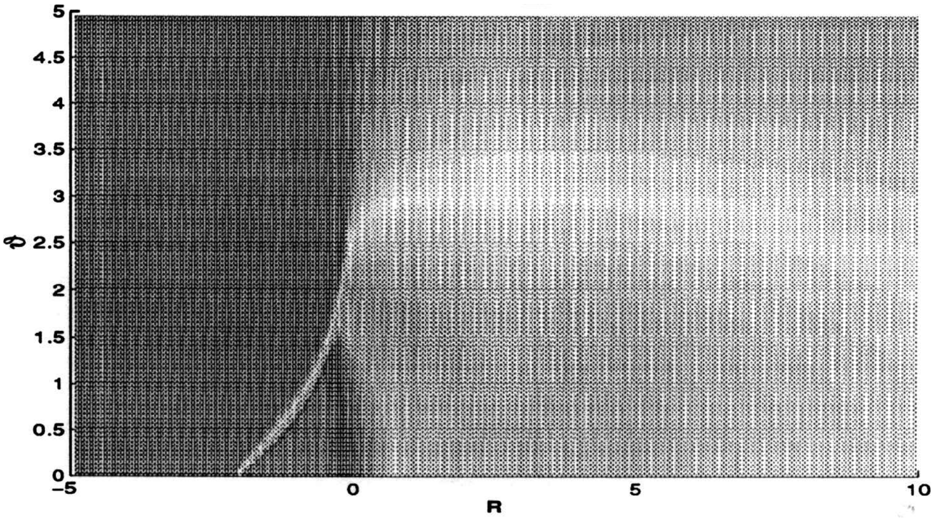

Fig. 7 Pressure coefficient contours in conical variables: $K = -4$.

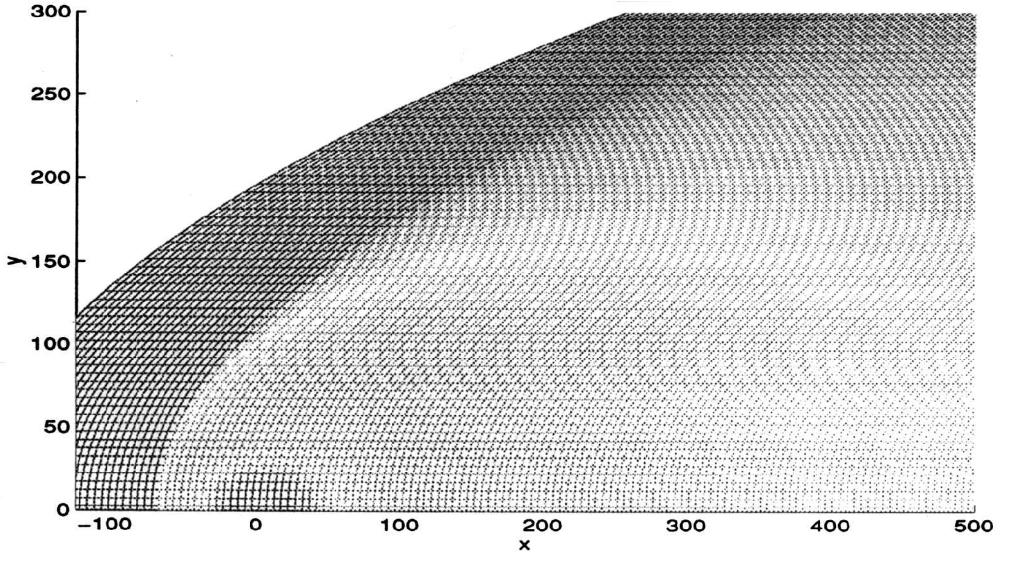

Fig. 8 Pressure coefficient contours in physical variables: $K = 1$ and $t = 100$.

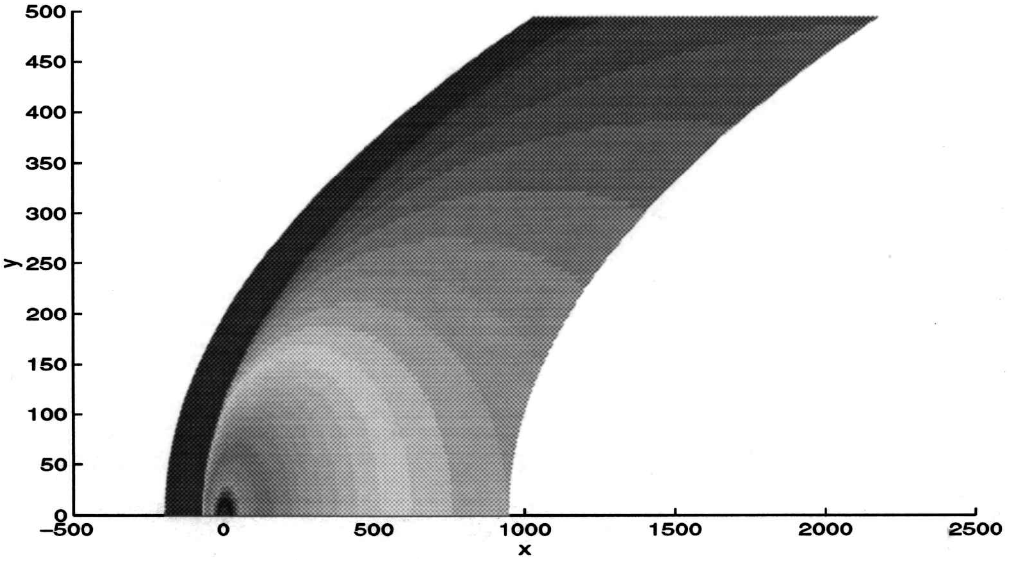

Fig. 9 Pressure coefficient contours in physical variables: $K = 1$ and $t = 100$.

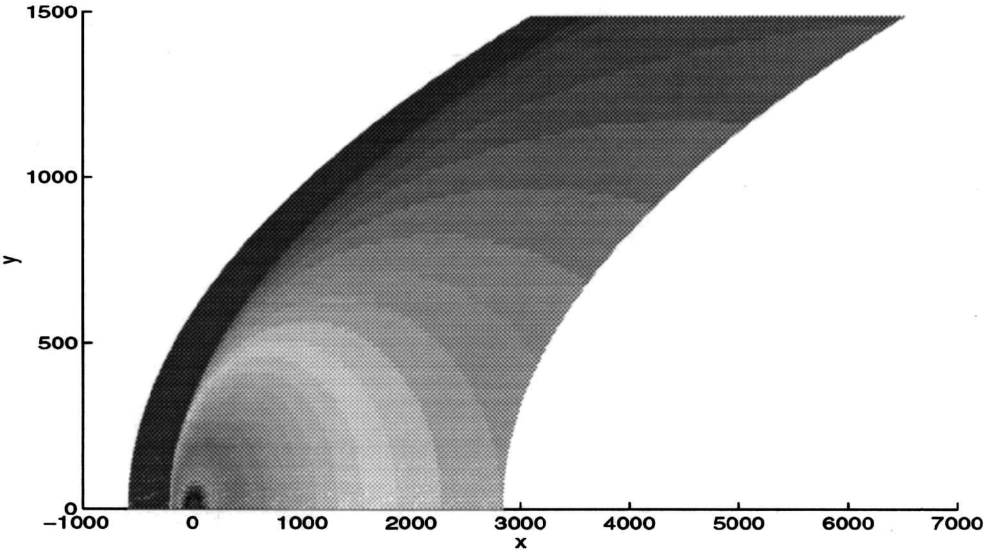

Fig. 10 Pressure coefficient contours in physical variables: *K* = 1 and *t* = 300.

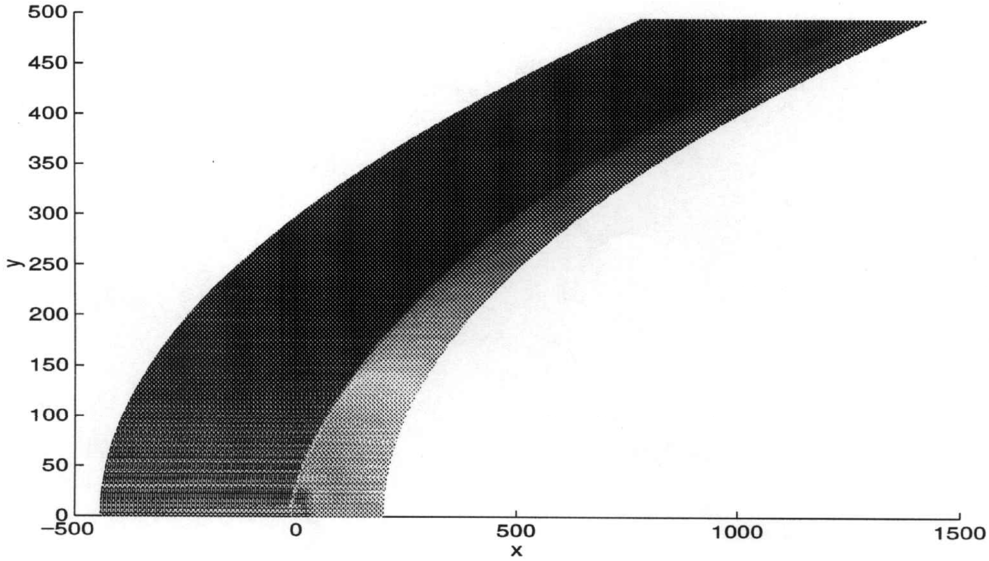

Fig. 11 Pressure coefficient contours in physical variables: *K* = _1 and *t* = 100.

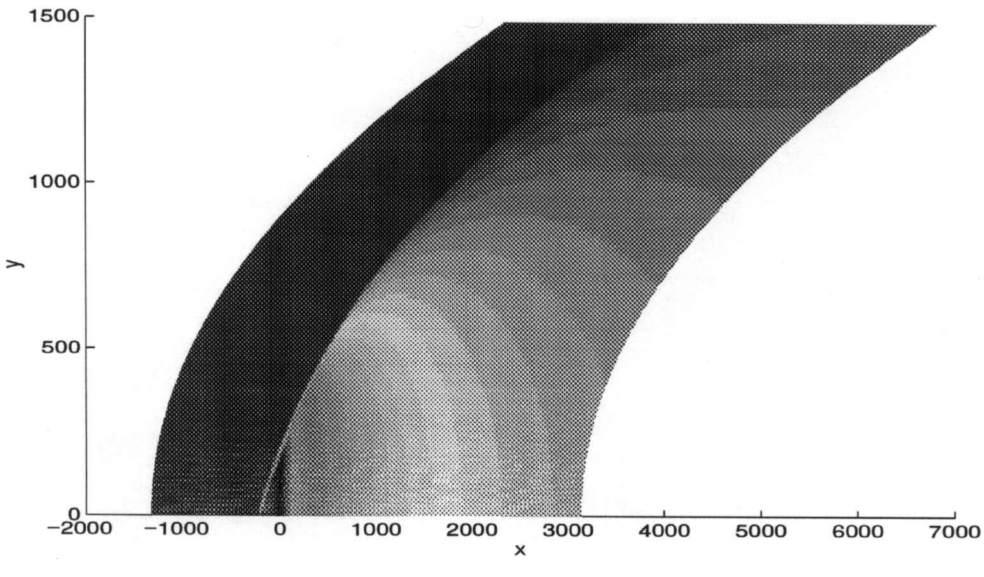

Fig. 12 Pressure coefficient contours in physical variables: *K* = _1 and *t* = 300.

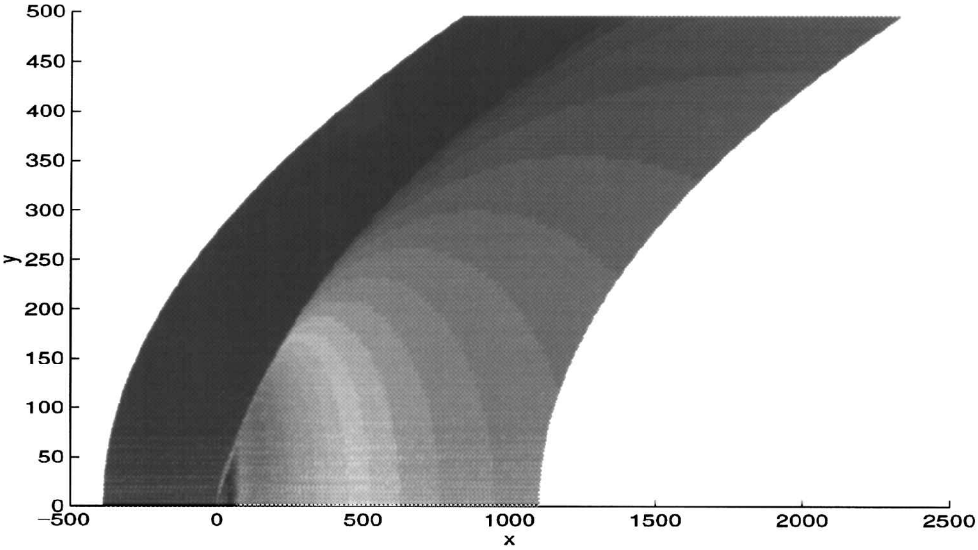

Fig. 13 Pressure coefficient contours in physical variables: K = _2.134 and t = 100.

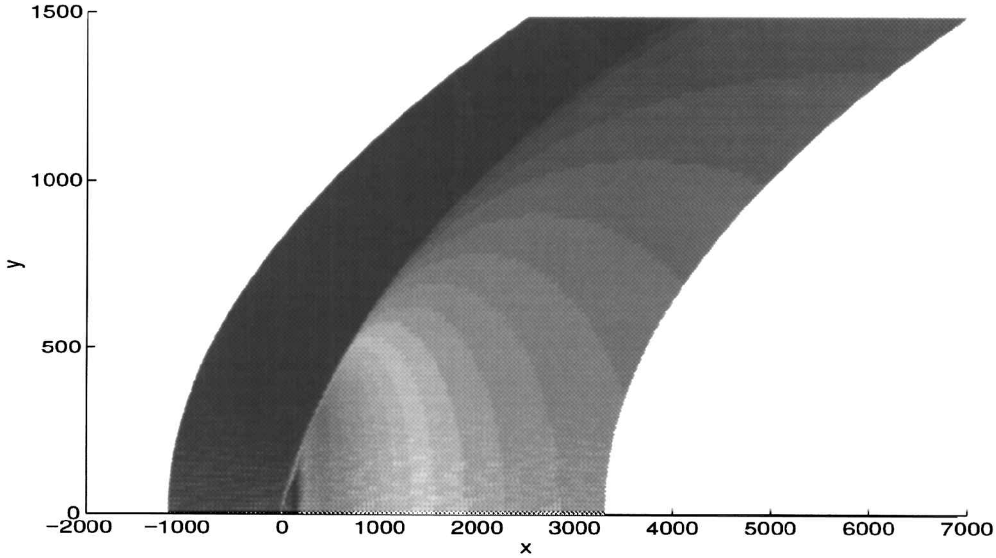

Fig. 14 Pressure coefficient contours in physical variables: K = _2.134 and t = 300.

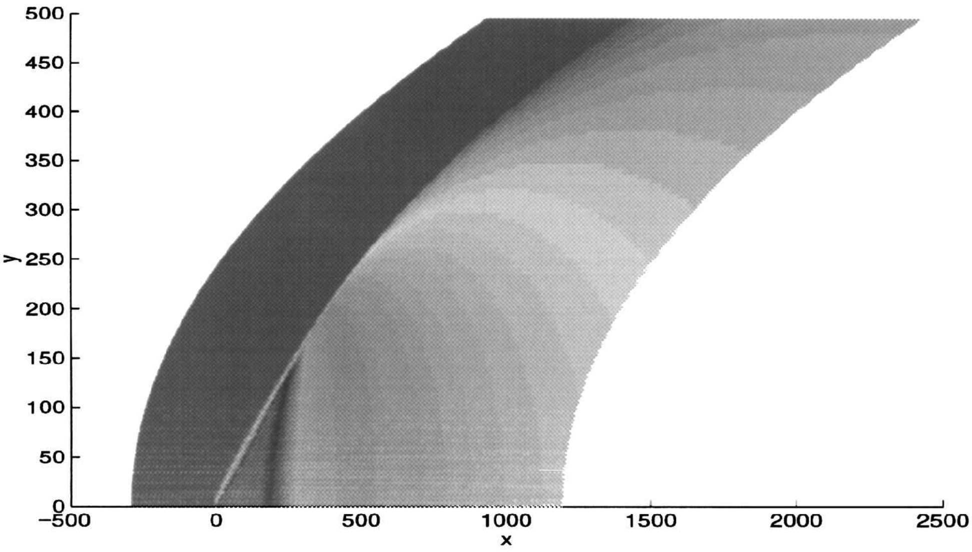

Fig. 15 Pressure coefficient contours in physical variables: K = _4 and t = 100.

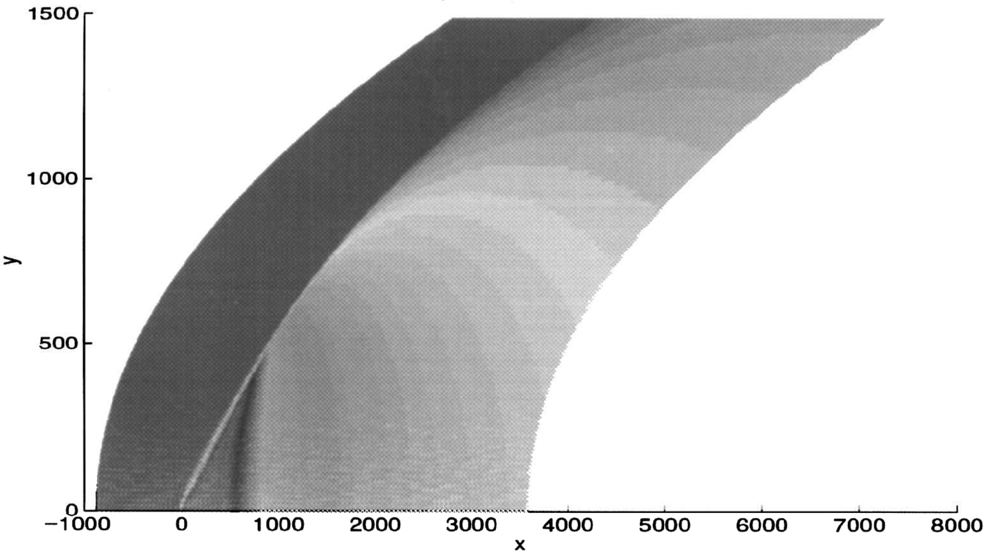

Fig. 16 Pressure coefficient contours in physical variables: $K = -4$ and $t = 300$.

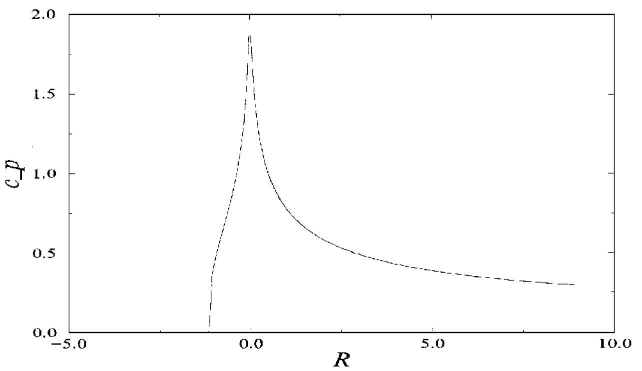

Fig. 17 Pressure coefficient on the wedge in conical variables: $K = 2$.

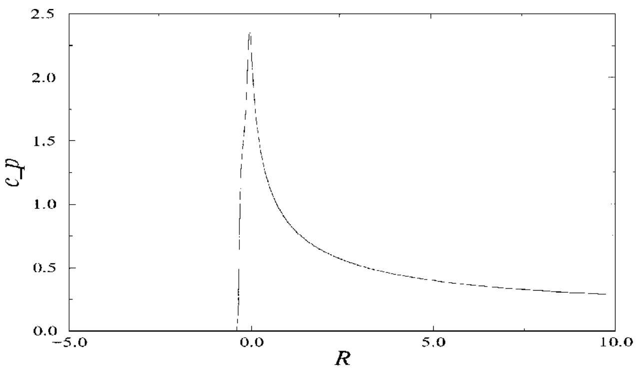

Fig. 18 Pressure coefficient on the wedge in conical variables: $K = 0$.

The plots have been executed for a range of values of K, namely -4, -2.134, -1, 0, 1, and 2. The value $K = -(3\sqrt{3}(\gamma+1)/4)^{2/3} \approx -2.134$ is that at which, for steady flow over the wedge, the flow behind the shock would be sonic. For $K > -2.134$, the steady flow would have a detached shock wave. At $K = -2.134$, the shock would attach itself to the wedge, but for $K > -2.258$, the flow behind would be subsonic; hence, the shock curved. The value $K = -[\sqrt{2}(\gamma+1)]^{2/3} \approx -2.258$ is that at which, for steady flow past the wedge, the shock straightens. Hence, for $K = -4$, the steady flow would have an attached, straight shock.[1] In addition to R, ϑ plots (which contain all of the $\tilde{x}$, $\tilde{y}$, t information), explicit ones in $\tilde{x}$, $\tilde{y}$ coordinates were done for $t = 100$ and $t = 300$.

Figures 3–7 show the pressure coefficient c_p at each point in R, ϑ space for the K values of -4, -2.134, -1, 0, 1, and 2 (note that the nose of the wedge, $x = y = 0$, corresponds to $R = K/2$, $\vartheta = 0$). The shock forms initially near the nose and, for $K > -2.134$, as time passes, it moves to upstream infinity. This is easily seen in Figs. 9–12, where the pressure is plotted in physical $\tilde{x}$, $\tilde{y}$ coordinates for a sequence of increasing times (note that Fig. 8 is a zoom in to show details of Fig. 9). The strength of the shock increases as K decreases, as can be seen more clearly from Figs. 17 and 18, which show the pressure coefficient on the surface ($\vartheta = 0$). The shock itself, for a fixed value of $K > -2.134$, not only moves upstream as t increases but also straightens (see Figs. 9–12 and note the different scales). This is expected because, for a fixed t, the shock asymptotes the parabola $\tilde{y}^2 = 2\tilde{x}t + Kt^2$ for large values of $\tilde{y}$. For $K \leq -2.134$, the shock is attached at the nose and stays that way. For $K \equiv -2.134$, it is curved; for $K = -4$, it is straight (Figs. 13–16).

Acknowledgments

This work was partially supported by Grant F49620-93-1-0022DEF from the Air Force Office of Scientific Research and Grant DMS-9210467 from the National Science Foundation.

References

[1] Cole, J. D., and Cook, L. P., *Transonic Aerodynamics*, North-Holland, New York, 1986.

[2] Cole, J. D., Cook, L. P., and Schleiniger, G., "An Unsteady Transonic Flow," *Zeitschrift für Angewandte Mathematik und Mechanik*, Vol. 76, Supplement 4, I–XII, 1996, pp. 525–528.

[3] Cole, J. D., Cook, L. P., Schleiniger, G., and Sinha, M., "Transonic Flow About a Suddenly Deflected Wedge," *Mathematics Is for Solving Problems*, Society for Industrial and Applied Mathematics, Philadelphia, PA, 1996, pp. 133–146.

[4] Schleiniger, G., "Quasi-transonic Flow Past Delta Wings," *Quarterly of Applied Mathematics*, Vol. 45, No. 2, 1987, pp. 265–277.

A. Plotkin
Associate Editor